Journal of Molecular Graphics and Modelling 61 (2015) 102–106

Contents lists available at ScienceDirect

Journal of Molecular Graphics and Modelling

journal homepage: www.elsevier.com/locate/JMGM

Revisit of polystyrene-modified fullerene core stars: A computational study

Jia Zhou [a,b,*]

[a] Department of Chemistry, Harbin Institute of Technology, Harbin 150001, China
[b] Center for Nanophase Materials Sciences, Oak Ridge National Laboratory, Bethel Valley Road, Oak Ridge, TN 37831-6493, United States

ARTICLE INFO

Article history:
Received 9 March 2015
Received in revised form 25 May 2015
Accepted 29 June 2015
Available online 7 July 2015

Keywords:
DFT
Fullerene
Arm-grafted
Polymer
Electronic effect
Steric effect

ABSTRACT

Density functional theory (DFT) calculations have been used to clarify the number of poly(styryl) lithium anions that are grafted onto C_{60} fullerene. The computational results suggest that 6-arm-grafted C_{60} fullerene is the most thermodynamically favorable, and the grafted C_{60} fullerene with arms more than 6 is only achievable under certain circumstances. This observation is consistent with the previous experiments [Macromolecules 2013; 46:7451–57.]. Both electronic effect and steric effect have been thoroughly examined and they are found to play different roles in the arm-grafted C_{60} fullerene. The current study will pave a way for the future architecture of polymers on C_{60} fullerene and the like.

1. Introduction

Since C_{60} fullerene was first detected in 1985 [1], its physical and chemical properties have been extensively investigated [2]. It is particularly interesting to incorporate C_{60} fullerene with a polymer matrix because it combines both the unique electronic properties of C_{60} fullerene and the well-known advantages of polymers in a single material. However, the poor solubility and incompatibility of C_{60} fullerene in polymers make such materials difficult to have practical applications.

As a multifunctional core molecule, C_{60} fullerenes have been used for the preparation of star-shaped polymers by grafting polymer or copolymer chains, in order to overcome the incompatibility between C_{60} and most polymers [3–7]. In 1992, Samulski and coworkers reported the reaction of poly(styryl) lithium (PSLi) with C_{60} fullerenes [3]. The experiments suggested that with the ratio of PSLi to C_{60} growing, the molecular weight of the product also increased, and the maximum number of arms is somewhere between 4 and 10. However, it had also been pointed out in the meantime by the authors that the Size Exclusion Chromatography (SEC) had the inherent limitations to characterize branched materials. Years later, Ederle and Mathis produced narrow monomodal C_{60} core stars under the high purity conditions when C_{60} was reacted with either PSLi or poly(isoprenyl) lithium (PILi) in nonpolar solvents, such as toluene [4]. Determined by SEC coupled with Light Scattering (LS), the maximum number of grafted chains per C_{60} core was found to be six for both PSLi and PILi. The limitation to six grafted arms is attributed to the charge delocalization of the six carbanions on the six pyracyclene units of the C_{60} core, resulting in the less favorable addition of more than six arms owing to the strong Coulombic repulsion between negative charges on the same pyracyclene unit [6]. However, very recent experiments by temperature gradient interaction chromatography (TGIC) [8–14] observed the C_{60} core stars with greater than six arms [15].

Although there have been plentiful studies on the arm-grafted C_{60} fullerene both experimentally and theoretically [3–8,15–17], several questions still remain: why 6-arm-grafted C_{60} core star is observed in every experiments with the most abundance; why greater than 6-arm-grafted C_{60} core star is only observed by the latest experiments; how the arms are grafted on C_{60} fullerene. In this work, we aim to systematically study the relationships between the grafted arms and C_{60} fullerene by DFT calculations. Different strategies will be adopted to build the arm-grafted C_{60} core star model. Thermodynamic results, alongside molecular orbital correlation, will be discussed for a thorough explanation on the experimental observations, in hope for providing guidance for future utilization of arm-grafted C_{60} core star.

* Correspondence to: Department of Chemistry, Harbin Institute of Technology, Harbin 150001, China.
E-mail address: jiazhou@hit.edu.cn

http://dx.doi.org/10.1016/j.jmgm.2015.06.014
1093-3263/

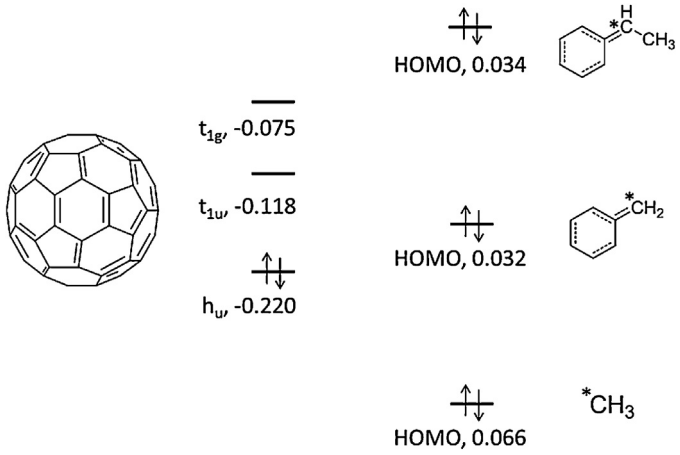

Fig. 1. HOMO, LUMO, and LUMO+1 of C_{60} calculated at the B3LYP/6-31G(d) level of theory using Gaussian 09 [26], and HOMO of different model arms with orbital energy (a.u.) calculated at the B3LYP/6-31++G(d,p) level of theory; asterisk indicates where the lone pair electrons (HOMO) mainly locate.

2. Methods

DFT calculations were performed using the Vienna *ab initio* simulation package (VASP) [18–21], unless stated otherwise. The Kohn–Sham equations were solved using the projector-augmented wave (PAW) method [22,23] with the Perdew-Burke-Ernzerhof (PBE) exchange and correlation functional [24,25] within the generalized gradient approximation. Each structure was enclosed in a supercell with a size of $30 \times 30 \times 30$ Å^3, large enough to ensure a separation from its periodic image by at least 10 Å. A kinetic energy cutoff of 400 eV was used for the plane-wave basis set. The Γ-point only sampling was used to describe the wave functions. The convergence criterion for the electronic self-consistent loop was set to 10^{-5} eV. During the structural optimizations, the lattice vectors of the supercell were fixed while all atoms were fully relaxed until the Hellmann-Feynman forces acting on them were smaller than 0.01 eV/Å. The above computational setups have been validated in our previous work [15]. The final energies of the ion-electronic systems were used to calculate the total binding energies (TBEs) and the differential binding energies (DBEs) according to:

$$\mathrm{nPS^-\,(arm) + C_{60}\,(core) \rightarrow (PS)_nC_{60}^{n-}\,(n\text{-arm star})},$$
$$\mathrm{TBE = E\,(n\text{-arm star}) - nE(arm) - E(core)} \quad (1)$$

$$\mathrm{PS^-\,(arm) + (PS)_{n-1}C_{60}^{(n-1)-}\,((n-1)\text{-arm star})} \rightarrow \mathrm{(PS)_nC_{60}^{n-}\,(n\text{-arm star})}, \quad (2)$$

$$\mathrm{DBE = E(n\text{-arm star}) - E(arm) - E((n-1)\text{-arm star})}$$

3. Results and Discussion

The real system is $(PS)_nC_{60}Li_n$, which is formed upon each subsequent addition of PSLi to C_{60}. However, the real system is too large to perform *ab initio* calculations. To this end, we adopted similar simplifications as those in our previous work [15]. Briefly speaking, the arms (PS) are modeled by small organic groups, such as methyl (Me), $C(C_6H_5)H_2$ (also as $CPhH_2$), and CPhMeH. It should be noted that these organic groups are all mono-anionic. These organic groups and C_{60} are shown in Fig. 1, along with the relevant orbitals (HOMO: highest occupied molecular orbital; LUMO: lowest unoccupied molecular orbital). On the other hand, Li^+ counterions are treated implicitly by adopting a homogeneous background charge ($+n$) in the calculation, depending on the magnitude of the negative charge ($-n$) present on the anionic species, $(PS)_nC_{60}{}^{n-}$. The implicit treatment of counterions is a reasonable choice in light of the salt nature of the core star anions which may remain dissociated as an electrolyte.

It is the central issue which carbon atoms of C_{60} the arms will attach. Two strategies will be discussed in the following. The first one is called "Consecutive", short as "C", and the other is called "Rearrangeable", short as "R". The basic assumption for both ideas is that the arms tend to minimize the steric repulsion from each other. Even though relatively small organic groups were used in our current study, it should be noted that the real arms (PS) are long chains, and thus steric constraint is quite significant. The difference between the two ideas is that for "C", the N-th arm attaches the position with the minimum steric repulsion from all the previous N-1 arms, and will not move once it has bound to C_{60}; while for "R", all the N arms will be allowed to adjust to minimize the steric repulsion. In mathematics, this comes to the aim of maximizing the distance between the attached carbon atoms of C_{60}. We also assume that C_{60} maintains I_h symmetry during the model building, which avoids the complexity caused by the arms, and makes the modeling more straightforward.

Figs. 2 and 3show the position/positions of C_{60}, labeled in red, which the arm/arms will attach for "C" and "R", respectively. Since carbon atoms of C_{60} are all identical, we just simply select one of them to start with. Considering the center of C_{60} buckyball, the 2nd carbon atom is in the opposite position to the 1st one, like a linear molecule. "C" and "R" begin to be different from $N = 3$. For "C", these three carbon atoms form T-shape geometry, while for "R", they are nearly trigonal planar. It should be reminded that C_{60} buckyball is not a perfect sphere, so carbon atoms are not always in the ideal positions in geometry. When $N = 4$, the four carbon atoms are almost square planar for "C", but tetrahedral for "R". For "C" at $N = 5$, the five carbon atoms form square based pyramidal geometry, as the 1st - 4th carbon atoms on the same equatorial plane, and the 5th atom sitting on the polar point. For "R", on the other hand, the five carbon atoms could be seen in two ways: either pseudo trigonal bipyramid if taking **a**/**b** or **c**/**d** in the axial positions and leaving the other three on the equatorial plane, or more distorted square based pyramid than in "C" if taking **e** in the apical position. "R" and "C" happen to be the same at $N = 6$, as octahedral geometry. It is easy to understand the way to build those of $N > 6$ for "C" from the octahedral geometry of $N = 6$. It is mono-capped octahedral geometry for $N = 7$, up to quadruple-capped octahedral geometry for $N = 10$. The even-numbered carbon atoms are always in the opposite position to its precedent odd-numbered atom. It is interesting at $N = 12$: one set of six carbon atoms comes from an outer conjunct circle of one six-membered ring, and anti-symmetric to the other respective set. For "R" at $N = 7$, the seven carbon atoms form pseudo pentagonal bipyramid, as the **a**/**b** carbon atoms in the axial positions, and the other five atoms approximately on the equatorial plane. For $N = 8$, it is a distorted square antiprismatic geometry: **a**/**b**/**c**/**d** on the same plane, and **e**/**f**/**g**/**h** on the other plane. For $N = 9$, it is close to capped square antiprismatic geometry, derived from $N = 8$ with the **i** carbon atom in the apical position. Similarly, it is bicapped square antiprismatic geometry for $N = 10$, with the **i**/**j** carbon atom in the apical position. It is a distorted icosahedron for $N = 12$, while for $N = 11$, it is the combination of half of $N = 10$ (**a**/**b**/**c**/**d**/**j**) and half of $N = 12$ (**e**/**f**/**g**/**h**/**i**/**k**).

Based on the strategies discussed above, different arm-grafted C_{60} core stars have been fully optimized, as shown in Supporting Information. Following Eqs. (1) and (2), the TBEs and DBEs were calculated from the total energies of the ion-electronic systems including mono-anionic arms (Me, $CPhH_2$, and CPhMeH), C_{60}, and $(arm)_nC_{60}{}^{n-}$ where n ranges from 1 to 12, as seen in Fig. 4 (the

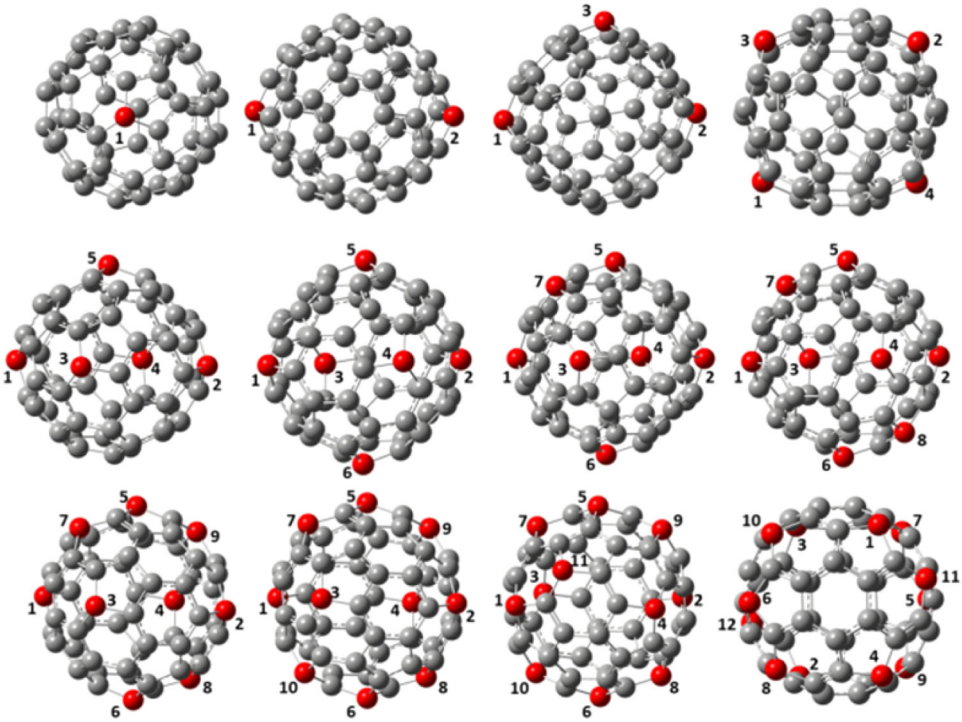

Fig. 2. Illustration of the positions (from 1 to 12) of C_{60} where arms consecutively attach.

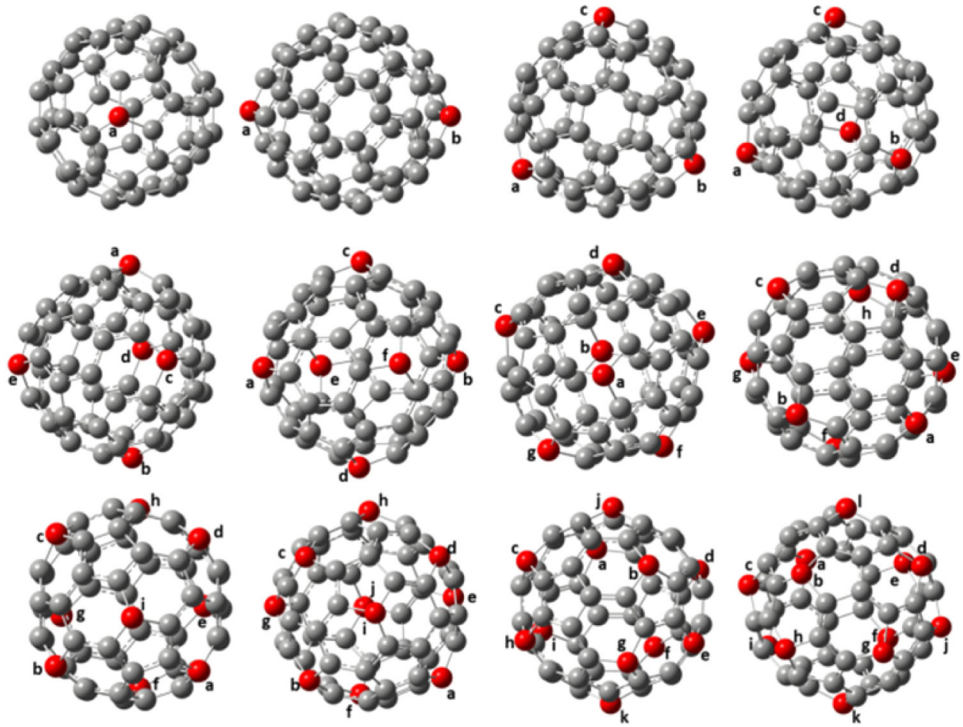

Fig. 3. Illustration of the positions (from a to l) of C_{60} where arms could rearrange after attachment.

data are also in Supporting Information). The solid blue curves in (a–c) are for "C" series, while solid red curves are for "R" series. It is interesting to see that for Me group, the TBE goes all the way down except for "R" at $N = 6$ and 7. Since Me group is very small, the steric repulsion is negligible here. The energy differences between "C" and "R" are all less than 20 kcal/mol with the only exception occurring at $N = 7$ by ca. 34 kcal/mol. In addition to $N = 1$ and 2, the energies between "C" and "R" at $N = 3$ and 4 are quite close within ca. 0.3 kcal/mol. It indicates that the positions of the arms do not matter significantly in energy when the arms are sparse relative to the C_{60} core. This phenomenon also holds for $CPhH_2$, and CPhMeH at $N = 3$ and 4, but with more steric repulsion due to the bigger arm size. Compared with Me group, $CPhH_2$ and CPhMeH groups are closer to the real system and more practical, with the latter even bigger in size. The phenyl (Ph) group helps to stabilize the lone pair of electrons in mono-anionic $CPhH_2$ and CPhMeH groups by

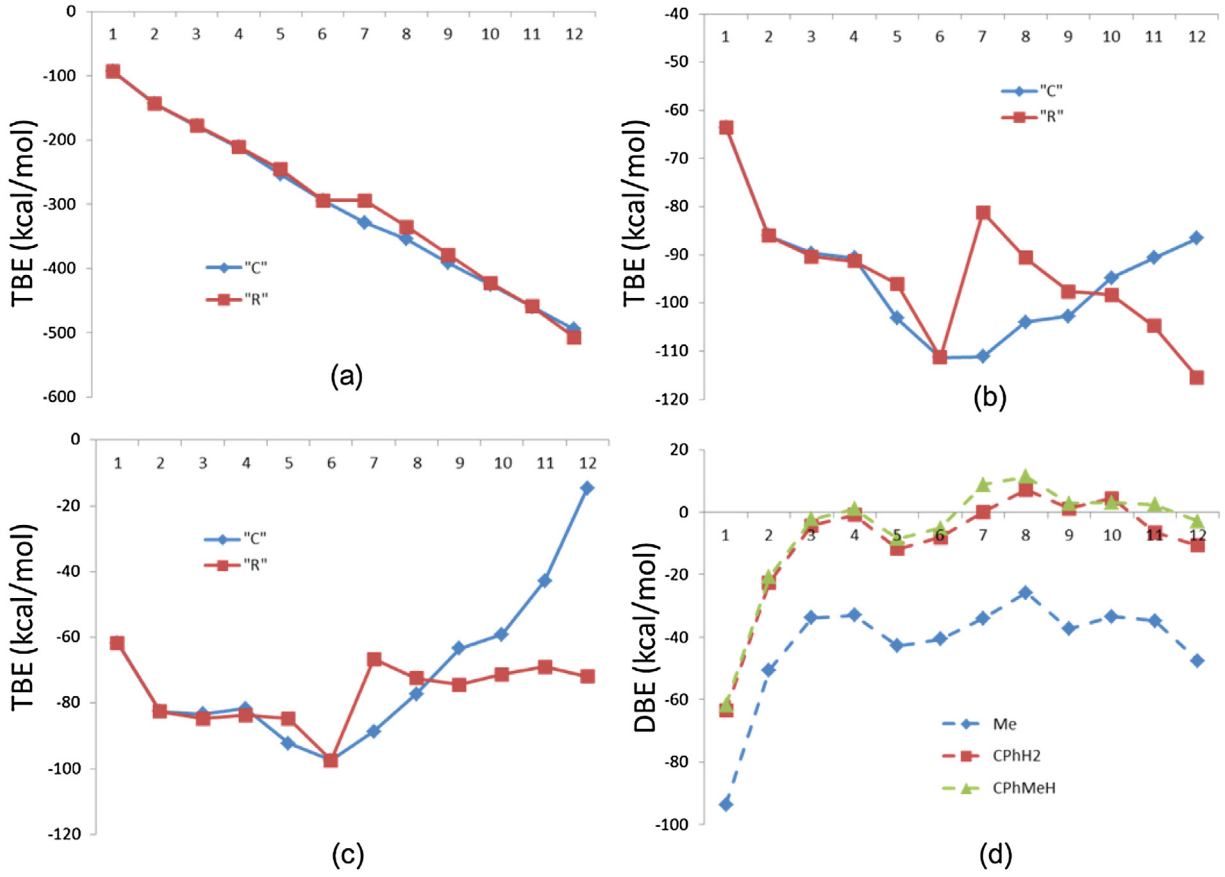

Fig. 4. The TBE (a: Me; b: $CPhH_2$; and c: CPhMeH) and DBE (d) as a function of the number of arms grafted onto C_{60}.

lowering the HOMO energy (these positive numbers are only for comparison purpose because counterions are omitted), as seen in Fig. 1. Therefore, $CPhH_2$ and CPhMeH mono anions are more likely to get free from PSLi to attack C_{60} than Me mono anion despite that the TBE of Me are much lower than those of $CPhH_2$ and CPhMeH. The "C" and "R" curves for $CPhH_2$ and CPhMeH groups are qualitatively similar. There is a clear minimum at $N = 6$ in the "C" curves for both of them. In the "R" curves, $N = 6$ is also a minimum, and $N = 7$ is a maximum. When the number of arms grows to some extent, the steric repulsion becomes more and more dominant, making the "R" conformation more favorable than its "C" counterpart. The critical point happens at $N = 10$ for $CPhH_2$ and at $N = 9$ for CPhMeH. Interestingly, even Me group also has this trend and the critical point is at $N = 12$, with 12.4 kcal/mol energy difference.

Between $N = 5$ and the critical point, the "C" conformation lies lower in energy than its "R" counterpart (too close at $N = 3$ and 4), particularly for $N = 7$. This indicates that steric repulsion does not play a dominant role in these cases. Our result shows that the TBE reaches the minimum at $N = 6$ on both "C" and "R" curves. This is consistent with the available experiments in which the 6-arm-grafted C_{60} fullerene is the most abundant. The reason for that comes from the symmetry of the molecules and corresponding molecular orbitals, as illustrated in Fig. 5. C_{60} fullerene is an I_h symmetric molecule, as a good electron acceptor. LUMO and LUMO+1 of C_{60} fullerene are of t_{1u} and t_{1g} symmetry, respectively, and both of them are of 3-folded degeneracy. Mono-anionic arms are electron donors, baring lone pair of electrons on carbon atom, as seen in Fig. 1. If only considering the lone pairs of the six arms, they form an O_h symmetric complex. As a result, these six orbitals could form two sets of orbitals, with t_{1u} and t_{1g} symmetry. The orbitals from C_{60} fullerene and arms with same symmetry could then correlate

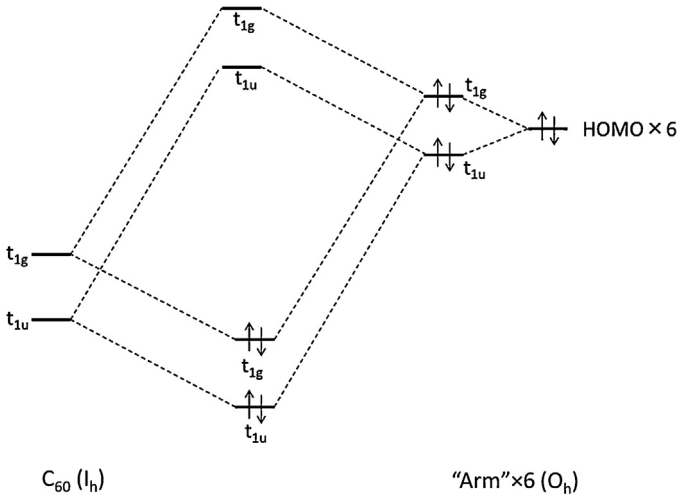

Fig. 5. Orbital correlation of C_{60} with six arms.

and form new orbitals. Six arms make LUMO and LUMO+1 of C_{60} fullerene fully occupied and maintain the symmetry to the largest extent. That explains not only why 6-arm-grafted C_{60} fullerene is the most abundant in the experiment, but also why its neighboring points prefer "C" conformation to "R". $N = 7$ is most apparent case for this matter. 7"R" breaks the aromaticity of C_{60} fullerene more significantly than 7"C", resulting in striking higher energy. Geometrically speaking, "R" conformation maximally minimizes the arm–arm repulsion, however *ab initio* calculations suggest "C" conformation lies significantly lower in energy. Even in the case of Me group, which is thought to have minimum steric repulsion

in both "R" and "C", "C" conformation edges "R" in energy by the most at $N = 7$. Therefore, we could come up with the conclusion that the arm-grafted C_{60} fullerene tend to maintain the most symmetric structure around $N = 6$. In other word, chemistry dominates geometry in these cases. Beyond these, the arms prefer the positions with minimum steric repulsion if possible.

If we select those structures with lower energy from both "C" and "R", and calculate the differential binding energies, it is the DBE curves in Fig. 4 (d). It is striking that the three curves of different arms are almost parallel, and the curves of $CPhH_2$ and CPhMeH are very close in particular at the beginning. Since there is no or little steric effect in Me case, the energy differences between the other curves and Me curve should largely come from steric effect. For the curves of $CPhH_2$ and CPhMeH, the first three points are all negative, indicating it is energetically favored to graft the first three arms. The 4th points are close to zero: −0.9 kal/mol for $CPhH_2$ and 1.0 kcal/mol for CPhMeH. The 5th and 6th points are negative again. Therefore, 4-arm-grafted C_{60} fullerene could be in equilibrium to some extent with 3-arm-grafted C_{60} fullerene, but inclines to draw more arms to form 5/6-arm-grafted C_{60} fullerene, which is exothermic again. This also explains why 5- and 6-arm-grafted C_{60} fullerene are among the most abundance in the experiment [15]. It then requires extra energy to grow bigger, so the content of 7-arm-grafted C_{60} fullerene and beyond decreases significantly. The extra energy could either come from the heat that the prior reactions produce or from the environment. It is noteworthy that $N = 9$ is another local minimum for all of the three curves, and close to zero, less than 3.0 kcal/mol. Therefore, it is expected that 9-arm-grafted C_{60} fullerene might be able to be generated if 8-arm-grafted C_{60} fullerene is formed, as is in accordance with the latest experiment as well [15]. On the other hand, 9-arm-grafted C_{60} fullerene could approximately be regarded as that the pseudo 3-folded degenerate LUMO of 6-arm-grafted C_{60} fullerene are again fully occupied. As mentioned previously that the positions of the arms do not matter significantly in energy when the arms are sparse relative to the C_{60} core, however the results of our model arms ($CPhH_2$ and CPhMeH) suggest that "C" TBE climbs monotonously from $N = 6$ on, with CPhMeH in a bigger slope. The real systems are even larger, so the arrangement of the arms is necessary for more arm-grafted C_{60} fullerene, and this probably occurs as early as $N = 8$.

4. Conclusions

In conclusion, this work has systemically studied the chemistry of anionically-modified C_{60} fullerene by DFT calculations. Two different strategies have been used to explore the grafted positions of the arms on C_{60} fullerene. When the number of the arms is relatively small ($N = 3, 4$), two strategies provide a similar result. It is confirmed that $N = 6$ is the most thermodynamically favorable, which is also well illustrated by molecular orbital correlation. For those around $N = 6$, the arm-grafted C_{60} fullerenes prefer "C" conformation. When the arms grow up to some points, the steric effect becomes dominant, making "R" conformation more and more favorable. The arrangement of the arms is necessary for amount of large arms to be grafted on C_{60} fullerene, although requiring extra energy, which is consistent with the latest experiment. Those investigations will undoubtedly guide the future experiments on arm-grafted C_{60} fullerene and the like.

Acknowledgment

This research was supported by the Fundamental Research Funds for the Central Universities (Grant No. AUGA5710013115), China and by the Center for Nanophase Materials Sciences, which is sponsored at ORNL by the Scientific User Facilities Division, U.S. Department of Energy. This work used computational resources of the National Center for Computational Sciences at Oak Ridge National laboratory and of the National Energy Research Scientific Computing Center, which are supported by the Office of Science of the U.S. Department of Energy under Contract No. DE-AC05-00OR22750 and DE-AC02-05CH11231, respectively. The author also thanks Dr. Huang at ORNL for helpful discussions.

Appendix A. Supplementary data

Supplementary data associated with this article can be found, in the online version, at http://dx.doi.org/10.1016/j.jmgm.2015.06.014

References

[1] H.W. Kroto, J.R. Heath, S.C. Obrien, R.F. Curl, R.E. Smalley, Nature 318 (1985) 162–163.
[2] H.W. Kroto, A.W. Allaf, S.P. Balm, Chem. Rev. 91 (1991) 1213–1235.
[3] E.T. Samulski, J.M. Desimone, M.O. Hunt, Y.Z. Menceloglu, R.C. Jarnagin, G.A. York, K.B. Labat, H. Wang, Chem. Mater. 4 (1992) 1153–1157.
[4] Y. Ederle, C. Mathis, Macromolecules 30 (1997) 2546–2555.
[5] D. Pantazis, S. Pispas, N. Hadjichristidis, J. Polym. Sci. A Polym. Chem. 39 (2001) 2494–2507.
[6] C. Mathis, B. Schmaltz, M. Brinkmann, C. R. Chim. 9 (2006) 1075–1084.
[7] B. Schmaltz, C. Mathis, M. Brinkmann, Polymer 50 (2009) 966–972.
[8] D. Berek, Prog. Polym. Sci. 25 (2000) 873–908.
[9] H.C. Lee, T. Chang, Polymer 37 (1996) 5747–5749.
[10] C.H. Lochmüller, M.A. Moebus, Q. Liu, C. Jiang, M. Elomaa, J. Chromatogr. Sci. 34 (1996) 69–76.
[11] P. Chambon, C.M. Fernyhough, K. Im, T. Chang, C. Das, J. Embery, T.C.B. McLeish, D.J. Read, Macromolecules 41 (2008) 5869–5875.
[12] S. Ahn, K. Im, T. Chang, P. Chambon, C.M. Fernyhough, Anal. Chem. 83 (2011) 4237–4242.
[13] X. Chen, M.S. Rahman, H. Lee, J. Mays, T. Chang, R. Larson, Macromolecules 44 (2011) 7799–7809.
[14] L.R. Hutchings, Macromolecules 45 (2012) 5621–5639.
[15] D. Uhrig, G.C. Morar, M. Goswami, J. Huang, B.G. Sumpter, J. Zhou, S.M. Kilbey, D.L. Pickel, Macromolecules 46 (2013) 7451–7457.
[16] F. Audouin, R. Nuffer, C. Mathis, J. Polym. Sci. A Polym. Chem. 42 (2004) 4820–4829.
[17] V. Weber, M. Duval, Y. Ederlé, C. Mathis, Carbon 36 (1998) 839–842.
[18] G. Kresse, J. Furthmüller, Comput. Mater. Sci. 6 (1996) 15–50.
[19] G. Kresse, J. Furthmüller, Phys. Rev. B 54 (1996) 11169–11186.
[20] G. Kresse, J. Hafner, Phys. Rev. B 47 (1993) 558–561.
[21] G. Kresse, J. Hafner, Phys. Rev. B 49 (1994) 14251–14269.
[22] P.E. Blöchl, Phys. Rev. B 50 (1994) 17953–17979.
[23] G. Kresse, D. Joubert, Phys. Rev. B 59 (1999) 1758–1775.
[24] J.P. Perdew, K. Burke, M. Ernzerhof, Phys. Rev. Lett. 77 (1996) 3865–3868.
[25] J.P. Perdew, K. Burke, M. Ernzerhof, Phys. Rev. Lett. 78 (1997), 1396–1396.
[26] M.J. Frisch, G.W. Trucks, H.B. Schlegel, G.E. Scuseria, M.A. Robb, J.R. Cheeseman, G. Scalmani, V. Barone, B. Mennucci, G.A. Petersson, H. Nakatsuji, M. Caricato, X. Li, H.P. Hratchian, A.F. Izmaylov, J. Bloino, G. Zheng, J.L. Sonnenberg, M. Hada, M. Ehara, K. Toyota, R. Fukuda, J. Hasegawa, M. Ishida, T. Nakajima, Y. Honda, O. Kitao, H. Nakai, T. Vreven, J.A. Montgomery Jr., J.E. Peralta, F. Ogliaro, M. Bearpark, J.J. Heyd, E. Brothers, K.N. Kudin, V.N. Staroverov, R. Kobayashi, J. Normand, K. Raghavachari, A. Rendell, J.C. Burant, S.S. Iyengar, J. Tomasi, M. Cossi, N. Rega, N.J. Millam, M. Klene, J.E. Knox, J.B. Cross, V. Bakken, C. Adamo, J. Jaramillo, R. Gomperts, R.E. Stratmann, O. Yazyev, A.J. Austin, R. Cammi, C. Pomelli, J.W. Ochterski, R.L. Martin, K. Morokuma, V.G. Zakrzewski, G.A. Voth, P. Salvador, J.J. Dannenberg, S. Dapprich, A.D. Daniels, Ö. Farkas, J.B. Foresman, J.V. Ortiz, J. Cioslowski, D.J. Fox, Gaussian 09, Gaussian, Inc., Wallingford, CT, 2009.